AIChE WILEY InterScience DISCOVER SOMETHING GREAT

PARTICLE TECHNOLOGY AND FLUIDIZATION

Wave Propagation and Granular Temperature in Fluidized Beds of Nanoparticles

Michael Driscoll and Dimitri Gidaspow
Dept. of Chemical and Environmental Engineering, Illinois Institute of Technology, Chicago, IL, 60616

DOI 10.1002/aic.11178
Published online May 14, 2007 in Wiley InterScience (www.interscience.wiley.com).

The speeds of motion of compression waves through a fluidized bed of 10 nm silica particles were determined by measuring the times of arrival of compression zones using a light probe. A correlation for the modulus of elasticity was determined as a function of void fraction. Using a kinetic theory type equation of state for particles, this experimentally determined modulus gives a value for the granular temperature for 10 nm particles of approximately one (meter per second) squared. This value is close to that obtained by assuming the motion of the 10 nm particles to be due to collision with air molecules with no energy dissipation. The values of the granular temperature were also determined in a two-dimensional (2-D) fluidized bed by measuring the volume fraction distributions of 10 nm silica particles. Granular temperatures were deduced from a one-dimensional particle momentum balance using an ideal equation of state for particles, which is similar to the barometric formula for gases. These granular temperatures agreed with the measurements obtained from wave propagation experiments. © 2007 American Institute of Chemical Engineers *AIChE J,* 53: 1718–1726, 2007
Keywords: nanoparticle, fluidization, wave propagation, granular temperature, nanotechnology, fluidization, fluid mechanics, particulate flows

Introduction

Nanoparticles have some unique flow properties that may be useful for a number of applications. Nanoparticles fluidize without the formation of bubbles. Since nanoparticles are light and have a large surface area when coated with metals by say, vapor deposition, they can serve as catalysts, which may compete, with traditional FCC particles to convert oil into gasoline. Jiradilok et al.[1] and Kalra[2] reported the viscosity of nanoparticles to be equal to half that of water. If nanoparticle metal hydrides are produced, they could be used as a fuel in fuel cells, greatly increasing the fuel-cell power density. The nanoparticles could then be fed into a fuel tank just like gasoline. Individual nanoparticles have the unique ability to be able to pass through cell membrane walls due to their small size enabling pharmaceutical drug delivery to more accurately target viruses or malignant cells.[3] Nanoparticles can also form micronsized agglomerates. The larger agglomerate size aids in the separation of the particles from the bulk fluid stream during processing.

Past research has provided several important insights into the properties of fluidized nanoparticles systems. Chaouki et al.[4] recognized the deviation of nanosized Cu/Al aerogel particles from Geldart Type C particle behavior. Chaouki et al. also documented the smooth fluidization characteristics (homogeneous-bed expansion) of the nanoparticle agglomerates, and utilized the Kunii-Levenspiel minimum fluidization velocity[5] correlation to estimate the agglomerate size. The agglomerate size was estimated at 700 microns vs. a measured agglomerate size of 1,000 microns. Wang et al.[6] evaluated the experimental fluidization of nine powders, including a 10 nm aerogel and 9 nm silica and noted the high-bed expansions, initial bed channeling, bubbleless fluidization, and the formation of 200–300 micron agglomerates. Yao et al.[7] experimentally fluidized six SiO_2 nanoparticles building on the work of Chaouki et al.[4] Transmission electron microscope (TEM) pictures of the agglomerates were presented. Agglomerate sizes were estimated

Correspondence concerning this article should be addressed to M. Driscoll at michael.driscoll@ge.com.

using the Richardson-Zaki equation. These calculations yielded agglomerate diameters that ranged from 230 to 330 microns. Li et al.[8] presented experimental, and limited simulations for $CaCO_3$ particles in a CFB. Limited entrainment due to agglomerate formation was observed at less than 1 m/s superficial-gas velocity. Jung and Gidaspow[9] used fluidization and collapsing bed experiments to determine the minimum fluidization velocity and solids-volume fraction for Tullanox nanoparticles in a 3-D bed. A two-fluid simulation model was developed assuming 18 micron heavy agglomerates. Bubbleless fluidization was observed. Zhu et al.[10] principally present an experimental study designed to evaluate the fluidization characteristics of 11 nanoparticles. An analytical method was developed to predict agglomerate size based on the Richardson-Zaki equation and Stokes Law. The calculated and experimentally measured agglomerate sizes were between 172 and 585 microns. Yang[11] discussed the cohesive forces that lead to the formation of agglomerates, the prediction of agglomerate size, and fluidization of nanoparticle agglomerates. At the recent Fifth World Congress on Particle Technology, Huang et al.[12] presented a summary of their nanoparticle fluidization research. In this work, measured dispersion coefficients for nanoparticles were presented. Pfeffer's Group also presented reports detailing the effect of gas viscosity on nanoparticle fluidization,[13] and an evaluation of methods to assist fluidization of nanoparticle systems.[14]

Extensive research has been performed to develop a simulation model that can predict the behavior of a fluidized gas-solid system. Sinclair[15] presented a summary of the many different solid-gas simulation models that had been developed including a summary of a two fluid model that utilizes the solids-stress modulus in the particulate momentum balance to numerically stabilize the convergence of the simulation. The solids stress modulus is a thermodynamic property of a solid particle,[16] and is defined by the following equation

$$\mathrm{G}(\varepsilon_s) = \left(\frac{\partial P_s}{\partial \varepsilon_s}\right)_{\mathrm{S\ or\ T}} \tag{1}$$

where G is the solids-stress modulus, P_s is the solids pressure, and ε_s is the solids-volume fraction.

Mutsers and Rietema[17] introduced the solids-stress modulus, initially called the elastic coefficient or modulus of elasticity, to explain the interparticle forces that maintain the structure of the fluidized bed during tilted bed experiments. Rietema and Piepers[18] mathematically related the solids-stress modulus to the wave-propagation velocity, and suggested the dependence of the solids-stress modulus on the void fraction of the fluidized bed. Gidaspow[16] provided the theoretical derivation of the solids-stress modulus from mass and momentum balances in a fluidized bed. Massoudi et al.,[19] Chen and Weinstein,[20] and Gelderbloom et al.[21] reviewed the background of various correlations for the solids-stress modulus. The correlations found in literature relating solids-stress modulus to void fraction were either synthesized from simulation results or obtained from experiments. Jung and Gidaspow[9] utilized settling experiments to obtain a relationship for the solids-stress modulus for 10 nm particles. They utilized this relationship to model the settling of fluidized nanoparticles in a 3-D bed.

Sinclair[15] also reviewed kinetic theory models that utilize the granular temperature (a measurement of the random oscillations of particles) in the energy-balance equations for a fluidized bed. The granular temperature in a fluidized bed has typically been measured by taking an average of the variance of the fluctuating velocity. Vasishta[22] and Kalra[2] determined the granular temperatures for three different nanoparticles in rectangular bed by solving the one-dimension momentum balance, and measuring the solids-volume fraction in a fluidized bed. Due to the formation of porous agglomerates, the fluidization of nanoparticles has been found to occur in the dilute regime. In the dilute regime, the particulate ideal state equation[16] can be applied, and the granular temperature in the riser determined in a relatively straightforward manner from the wave-propagation velocity through a fluidized bed.

In this article, we show that the hydrodynamic properties of a bed of fluidized nanoparticles are influenced by the random oscillations of the particles, the granular temperature. The results of a series of experiments, whereby a shock wave is introduced into the bottom of a fluidized bed, and a wave of compressed solids propagates through the bed are presented. This experiment will determine the granular temperature and the solids-stress modulus by measuring the characteristic velocity of the 1-D wave through the fluidized bed of nanoparticles. The characteristic velocity for fluidized particles is shown to be the sum of the bulk-solids velocity plus the oscillating velocity (or the square root of solids-stress modulus divided by the solids density)

$$\frac{dx}{dt} = v_s + v_{osc} = v_s + \sqrt{\frac{G}{\rho_s}} = v_s + \sqrt{G'} \tag{2}$$

For a stable-fluidized bed, with no net-solids velocity, this equation reduces to the following relationship

$$\frac{dx}{dt} = \sqrt{\frac{G}{\rho_s}} = \sqrt{G'} \tag{3}$$

For dilute solids where the particulate ideal state equation ($P_s = \rho_s \varepsilon_s \theta$) applies, it is shown in Appendix A that the characteristic velocity is also equal to the square root of the granular temperature (θ). Therefore,

$$\frac{dx}{dt} = \sqrt{\theta} = \sqrt{G'} \tag{4}$$

The detailed derivation of these equations is presented in Appendix A.

Experimental Riser Description

Based on critical flow theory relationships outlined in Gidaspow,[16] a series of experiments were developed to determine the granular temperature and the modified solids-stress modulus of a fluidized bed of nanoparticles. The experiments would consist of inducing a compression wave in the bottom of the fluidized bed, and measuring the time for the wave to traverse the bed to the sensor. The experimental setup is shown in Figure 1.

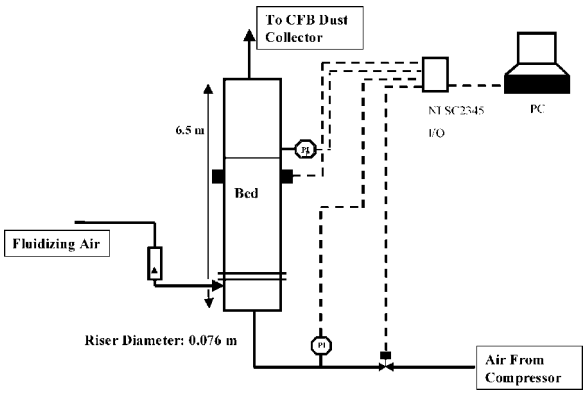

Figure 1. Riser experimental apparatus.

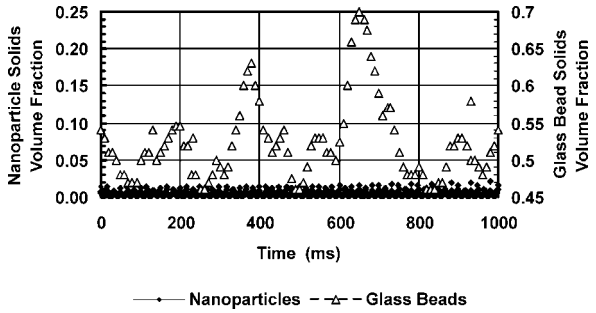

Figure 2. Nonbubbling behavior of 10 nm silica nanoparticles compared to 500 micron glass beads.

The experiment was initiated by adding a specific amount of Tullanox 500 nanoparticles to the riser. Tullanox 500 is fumed silica that has a typical particle size of ten nanometers. A constant flow rate of air is then injected into the riser to fluidize the particle bed, and the new fluidized height of the bed is recorded. The local solids-volume fraction of the fluidized bed is inferred by recording the voltage generated from a photovoltaic sensor, when a constant light source is passed through the fluidized bed. The riser is equipped with a high-intensity light source (a Fiber lite-A3200 with a 200 watt bulb). This light source provided a constant color, uniform light source with intensity control. The voltage generation cell was a high-speed borosilicate detector (Edmunds Optics model NT55-338 15 mm^2). The voltage generated by the detector is inversely proportional to the solids-volume fraction of the fluidized bed.[22,23,24] The voltage signal is collected using a National Instruments data collection system. The voltage signal is sent to a NI SCC-AI05 2 channel 100mv analog input module. This analog input module resides in a NI SC-2345 portable shielded module carrier. The NI SC-2345 is connected to a NI PCI-6221 M Series Multifunction DAQ card in the PC. The experimental data are collected and saved into an Excel spreadsheet utilizing Labview software.

Next, a quick acting valve at the bottom of the riser is actuated. This valve regulates a high-pressure source of air to the column. The valve is controlled by the personal computer. The PC simultaneously recorded the valve position and generated voltage signal. By recording the time the valve is opened, the time required for the solids wave to travel to the sensor, the distance to the sensor, and the solids-volume fraction of the bed, a correlation for the modified solids-stress modulus, or granular temperature vs. volume fraction can be developed.

Experimental Results

The solids-volume fraction in the riser was recorded using the light diode method described earlier. The solids-volume fraction signal showed very low-variability over the time data were collected. Figure 2 shows the short-term variability of the nanoparticle solids-volume fraction compared to that of a fluidized bed of 500 micron glass beads.[25] This graph shows that the range of the solids-volume fraction (SVF) for 500 micron glass beads (0.7–0.45) is more than 10 times greater than the range of the solids-volume fraction of the nanoparticles (0.015). The large range of the SVF for fluidized glass beads is due to the formation of bubbles in the fluidized bed. The tight range of the SVF for nanoparticles suggests that fluidization occurs without the formation of bubbles.

For each experiment, the inferred solids-volume fraction (voltage generated), and the position of the valve were recorded. A calibration curve was developed relating the voltage generated to the solids-volume fraction. The raw experimental results, voltage generated and valve position as a function of time are presented in Figure 3. This graph shows the voltage generation runs constant until slightly after the valve is opened. The voltage drops suddenly as the compression wave passes and then increases sharply as the gas surge dilutes the solids concentration. The voltage data were converted to solids volume fraction data via the calibration relationship. Figure 4 presents the solids-volume fraction and the valve position that correspond to this experiment. Once the valve was opened, the high-pressure air source induced a compression wave that propagated through the fluidized bed. The solids-volume fraction runs approximately constant for the first 5,000 ms then shows a sharp spike upward followed by a shift to a lower value. This graph shows the solids-volume fraction spikes shortly after the valve was opened, as the solids compression wave passes, and then decreases as the particles are blown through the bed. The time between the opening of the valve and the spike in the solids-volume fraction represents the time of arrival for the compression

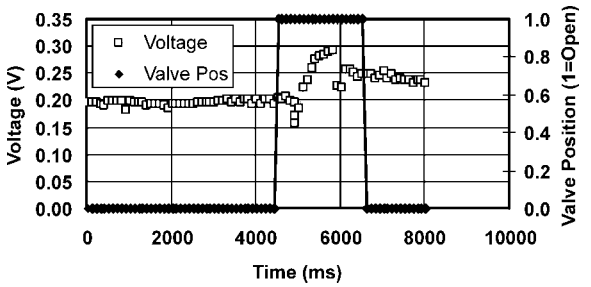

Figure 3. Cell voltage and valve position during wave propagation experiments.

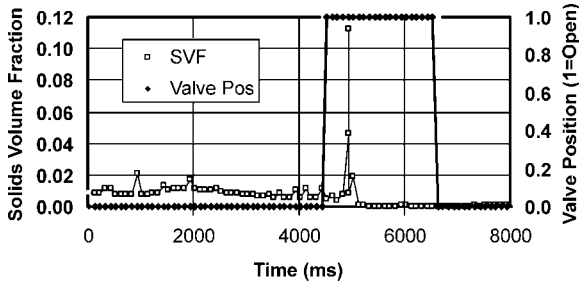

Figure 4. Riser solids-volume fraction and valve position during wave propagation experiments.

wave to travel to the sensor. Therefore, the first test yielded a wave velocity of

$$v_c = \frac{dx}{dt} \approx \frac{\Delta x}{\Delta t} = \frac{(0.71\ m)}{(4.95 - 4.46\ \text{sec})} = 1.44\ m/s \qquad (5)$$

The modified solids-stress modulus (G'), or granular temperature (assuming negligible solids velocity, since the fluidized-bed height remained constant prior to the induced wave) can be calculated as follows

$$G' = \frac{G}{\rho_s} = \theta = \left(\frac{dx}{dt}\right)^2 = (1.44\ \text{m/s})^2 = 2.07\ \text{m}^2/\text{s}^2 \qquad (6)$$

Now, this experimental process was repeated for several bed heights. The results for the experimental runs are summarized in Table 1. This table shows that the measured granular temperature ranged from 1 m^2/s^2 to slightly greater than 3 m^2/s^2. Figure 5 presents the granular temperature as a function of bed-void fraction for these experiments. This graph shows a causal relationship between granular temperature and void fraction. This graph shows that the granular temperature increases as the void fraction decreases (or as the solids-volume fraction increases).

Modified Solids Modulus Correlation

The data from the riser experiments were analyzed statistically to understand the causal relationship between the modified solids-stress modulus and the bed-void fraction. The following relationship between the modified solids-stress modulus and void fraction was determined via statistical analysis

$$G' = 10^{-58.6586\varepsilon + 58.4817} \qquad (7)$$

The relationship is statistically sound with a p-value of 0.002, and a R-Sq value of 92.1%. The correlation shows a causal relationship between the logarithm of G' and the void fraction and is presented in Figure 6. This equation is valid for the particle density (2200 kg/m^3). The correlation must be corrected for changes in agglomerate density.[23] In order to calculate the solids-stress modulus, G, the agglomerate density is required. Zhu et al.[10] measured the size of several SiO_2 agglomerates, and found the agglomerate diameter to range from 172 – 585 microns during agglomerate particulate fluidization. The authors further assumed that the agglomerate density remains constant during the complete fluidization process (yielding agglomerate densities ranging from 39–75 kg/m^3). Wang et al.[6] proposed a correlation for calculating agglomerate density for fine particles including SiO_2 nanoparticles. This correlation yields an agglomerate density that ranged from 74 to 222 kg/m^3, and agglomerates diameters that ranged from 100–300 micron. Finally, the agglomerate density was back-calculated from the Wen and Yu minimum fluidization correlation (using a minimum fluidization velocity of 1 cm/s measured by Jung and Gidaspow[9] and Vasishta[22] for Tullanox nanoparticles). This calculation yielded agglomerate densities that ranged from 335 to 750 kg/m^3 and agglomerate diameters that ranged from 200 to 300 microns. Based on this review, an agglomerate density of 200 kg/m^3 was assumed to compare this correlation to a past solids-stress modulus correlation. Figure 7 presents the comparison of the new correlation for the solids-stress modulus to the correlation proposed by Jung and Gidaspow.[16] This graph shows a similar trend for each correlation (as the void fraction decreases, the solids-stress modulus increases). These correlations are qualitatively consistent with each other although the experimental methods used to develop the correlations were very different.

The granular temperatures obtained with this experimental method are consistent with granular temperatures obtained in a rectangular bed. The methodology used to determine granular temperature in a rectangular bed is now presented.

Theoretical Background—Granular Temperature in a Rectangular Bed

The 1-D solids-momentum balance[16] assuming negligible acceleration, negligible wall friction, and zero average solids velocity is given by

$$\frac{dP_s}{dx} + g\varepsilon_s(\rho_s - \rho_g) = \beta_B v_g \qquad (8)$$

The momentum balance is based on a positive upward x-direction and gravity is directed negative in the downward direction (Figure 2.1 in Gidaspow[16]). In this equation, the drag force balances the solids pressure and the buoyant force.

Table 1. Wave Propagation Experimental Results

Bed Height (m)	H/Ho	t_o (s)	t_f (s)	dt (s)	dx (m)	V_c (m/s)	G' (m^2/s^2)	Void Fraction
1.09	2.53	4.48	4.88	0.40	0.7	1.77	3.12	0.9892
1.12	2.62	4.56	5.00	0.45	0.7	1.58	2.51	0.9896
1.46	3.41	4.46	4.95	0.49	0.7	1.44	2.07	0.9920
1.50	3.51	4.92	5.45	0.53	0.7	1.33	1.77	0.9922
2.15	5.02	4.39	5.01	0.63	0.7	1.13	1.27	0.9946
2.17	5.05	4.63	5.20	0.57	0.7	1.24	1.55	0.9946

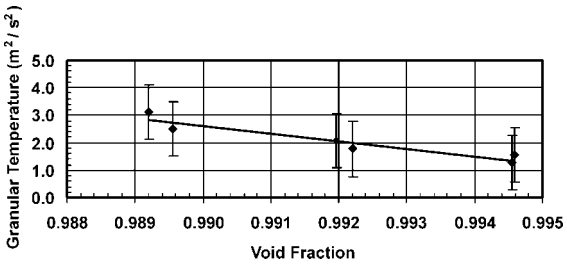

Figure 5. Riser granular temperature during wave propagation experiments.

Solids pressure can be expressed by the following relationship from the kinetic theory of granular flow[16]

$$P_s = \rho_s \varepsilon_s \theta \tag{9}$$

Now if one assumes constant granular temperature, substituting the ideal equation of state for granular flow into the previous equation yields

$$\rho_s \theta \frac{d\varepsilon_s}{dx} + g\varepsilon_s(\rho_s - \rho_g) = \beta_B v_g \tag{10}$$

This is a first-order differential equation. The solution to this equation is the sum of the homogeneous solution and a particular solution. The homogeneous solution to this equation is given by the following equation[22]

$$\varepsilon_s = A \exp\left\{-\frac{g}{\theta}\left(\frac{\rho_s - \rho_g}{\rho_s}\right)X\right\} \tag{11}$$

Now for the particular solution, a slightly different method vs. past research[2,22] is utilized. Recognizing that the average solids-volume fraction for the rectangular bed is a measurable quantity, the primary-differential equation is rearranged

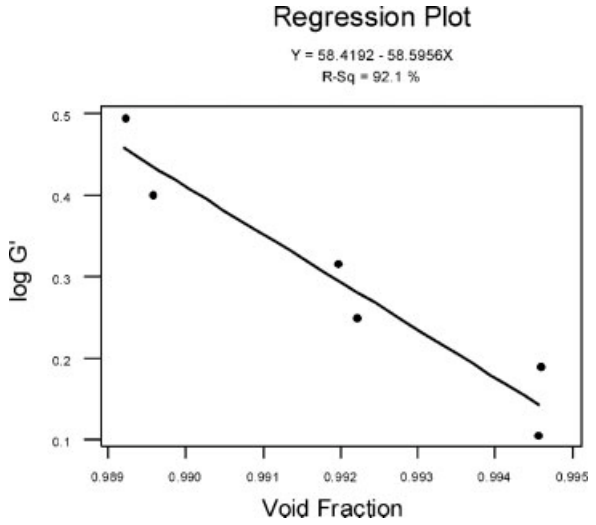

Figure 6. Fitted line plot for modified solids stress modulus vs. the void fraction.

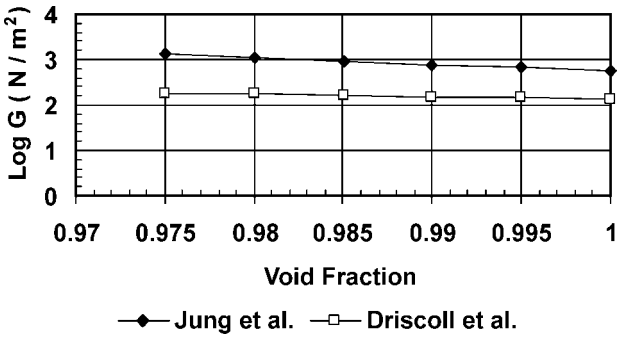

Figure 7. Comparison of the solids-stress modulus correlation for this study (assuming an agglomerate density equal to 200 kg/m^3) to the correlation from Jung and Gidaspow.[9]

to include the average solids-volume fraction as a term in the particular solution. Rearrangement of this equation yields

$$\frac{1}{L1}\int_0^{L1} \varepsilon_s dx = \varepsilon_{s,avg} = \frac{\beta_B v_g}{g(\rho_s - \rho_g)} - \frac{\rho_s \theta}{g(\rho_s - \rho_g)L1}(\varepsilon_{sL1} - \varepsilon_{so}) \tag{12}$$

Utilizing order of magnitude analysis on this equation reveals that the final term can be neglected for the nanoparticle system. Therefore,

$$\varepsilon_{s,avg} = \frac{\beta_B v_g}{g(\rho_s - \rho_g)} \tag{13}$$

Therefore, if the overall solids-volume fraction for the fluidized bed has been measured, we can use this value as the particular solution to the differential equation. The complete solution is the sum of the homogeneous and the particular solutions

$$\varepsilon_s = A \exp\left\{-\frac{g}{\theta}\left(\frac{\rho_s - \rho_g}{\rho_s}\right)X\right\} + \varepsilon_{s,avg} \tag{14}$$

Application of the boundary condition at $X = 0$, $\varepsilon_s = \varepsilon_{s0}$, and solving yields

$$A = \varepsilon_{s0} - \varepsilon_{s,avg} \tag{15}$$

Substituting this result into the complete solution, simplifying and rearranging yields the final solution for the differential equation

$$\mathrm{Ln}\left[\frac{\varepsilon_{s0} - \varepsilon_{s,avg}}{\varepsilon_s - \varepsilon_{s,avg}}\right] = \frac{g}{\theta}X \tag{16}$$

By using this relationship, the granular temperature may be calculated by utilizing experimental data containing the solids volume fraction as a function of fluidized bed height.

Rectangular Bed Experimental Description

Based on this theory, a series of experiments were conducted to better understand the hydrodynamic behavior of

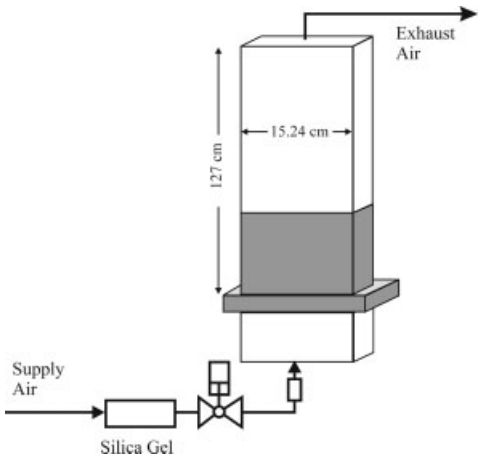

Figure 8. Rectangular bed.

nanoparticles in a rectangular bed. The fluidized bed used for these experiments is constructed of 0.635 cm plate glass with the inside dimensions of 2.54 cm deep by 15.24 cm wide by 127 cm tall. At the base of the rectangular glass bed is a fine 304L stainless steel wire support grid (165 × 1,400 mesh) that is used to support the particle bed. A gas distributor 17.78 cm tall is located directly below the support grid. Compressed air is conditioned prior to entering the fluidized bed. First, the air flows through a silica bed to remove water from the air stream. Next, the air is let down to 30 psig by a pressure regulator. Finally, directing the air stream through a rotameter with a manual valve regulates the airflow rate to the fluidized bed. Air from the fluidized bed is discharged to the atmosphere. A diagram of the rectangular bed is shown in Figure 8.

The solids-volume fraction in the fluidized bed was measured using the light diode assembly described previously. The fluidized bed was charged with Tullanox 500. Tullanox 500 is fumed silica that has a typical particle size of 10 nanometers. Nanoparticles tend to form agglomerates that are typically around 100–400 microns.[7,10,23] The calibration method was conducted by adding a small amount of Tullanox to the fluidized bed, recording the mass of material, volume of the fluidized bed, and the generated voltage. For each volume, an average of the several measurements at a given volume was taken as the representative voltage corresponding to the given solids-volume fraction. The bed was expanded to several different volumes by injecting fluidization air into the bed, and the data were recorded at each set of conditions, and a calibration curve was developed. The calibration curve is presented in Figure 9. This calibration procedure

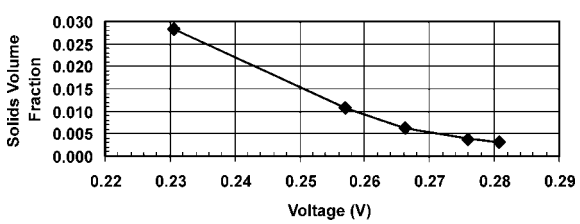

Figure 9. Calibration curve for rectangular bed.

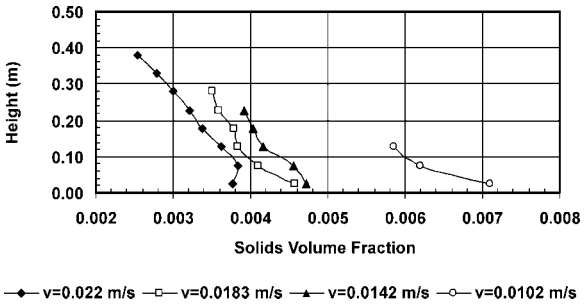

Figure 10. Fluidization of 10 nm Tullanox particles in a rectangular bed at various gas velocities.

established a representative voltage for each solids-volume fraction.

Rectangular Bed Experimental Data

Figure 10 shows the solids-volume fraction at various bed heights for four different gas velocities. The solids-volume fraction values presented in Figure 10 were determined from the voltage calibration curve. For all the trends, the solids-volume fraction is the higher at the bottom of the bed. Above the highest data point shown in Figure 10, there exists an abrupt density change. The visible bed height is located a few centimeters above the top data points. Vasishta[22] and Kalra[2] obtained similar trends using a different calibration procedure.

Rectangular Bed Granular Temperature

The results of these runs were used to calculate the granular temperature by the following relationship

$$\mathrm{Ln}\left[\frac{\varepsilon_{s0}-\varepsilon_{s,avg}}{\varepsilon_{s}-\varepsilon_{s,avg}}\right]=\frac{g}{\theta}X \tag{17}$$

Figure 11 presents the calculated granular temperature as a function of void fraction for all of these experiments. The granular temperature measured in the rectangular bed was relatively constant at 1 m^2/s^2 over the small range of gas velocities evaluated in this study.

These data show a strong relationship between the granular temperature and the fluidized-bed void fraction. The granular temperature for Tullanox has a similar shape and magnitude to the granular temperature curves from Vasishta[22] for R106 and R974. Figure 12 presents the granular temperature for both the riser and the rectangular bed as a function of void

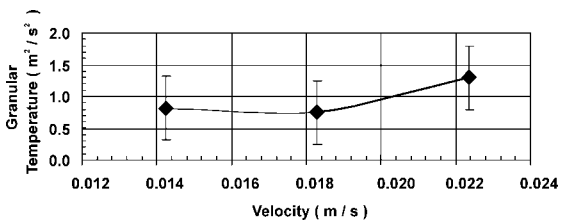

Figure 11. Granular temperature in a rectangular bed.

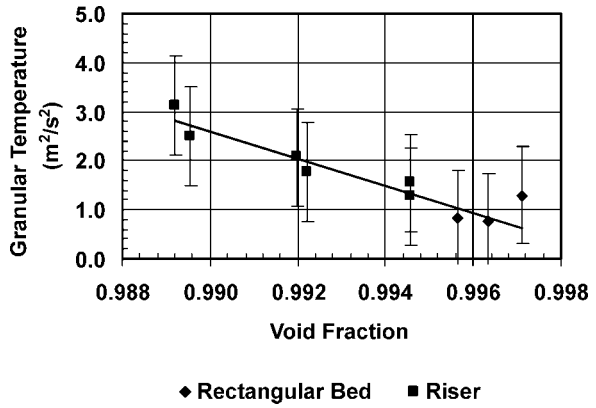

Figure 12. Granular temperature of nanoparticles in a vertical riser and in a rectangular bed.

fraction. This graph shows that granular temperature decreases as void fraction increases. The value of granular temperatures measured in the wave propagation experiments (1 m^2/s^2–3 m^2/s^2) is of the same order of magnitude as the granular temperatures reported for rectangular beds. These graphs show the granular temperature for Tullanox nanoparticles to vary linearly with void fraction.

Need for Solids-Stress Modulus in CFD Model

Two types of CFD models are used in modeling gas-particle flow and fluidization.[16] The first model type requires for its input the measured viscosity, and the solids-stress modulus for the particles. Jiradilok et al.[1] have used such a model to describe explosive dissemination of nanoparticles. The second type model is based on the kinetic theory. This advanced approach requires the calculation of the granular temperature from which the solids-stress modulus and the particle viscosity can be computed. The granular temperature equation (for example, Eq. 9.211 in Gidaspow[16]), shows that in such an equation the production of granular temperature is due to two mechanisms. The first is the production of fluctuations by shear. The second is the production due to fluid turbulence or due to collision with molecules. In the literature, several production terms due to fluid interaction have been proposed. Unfortunately, none of them accurately cover the complete range of particle sizes and flow regimes. They cannot currently be applied to nanoparticles. In this study, we see that the granular temperature for nanoparticle systems is principally due to the collision of air molecules with the nanoparticles (Figure 13). The production due to the shear is small for nanoparticles. In view of the lack of a complete kinetic theory applicable to nanoparticles we cannot, at present, use the kinetic theory approach.

Conclusions

This study presented a novel method to determine the granular temperature or the modified solids-stress modulus of a fluidized bed of nanoparticles. The granular temperatures measured ranged from approximately 1 m^2/s^2 to 3 m^2/s^2. These values are typical for Geldart type A particles. The data from these experiments were also used to develop a causal relationship between the modified solids-stress modulus and the void fraction. The relationship between solids-stress modulus and void fraction is needed for hydrodynamic modeling. In such a model, this solids-stress modulus, and the measured nanoparticle viscosity are inputs into the CFD model.[1]

The values of granular temperature from this study are close to the values computed, assuming the oscillations are due to nearly elastic collisions of nanoparticles with air molecules.[1] For fluidization of large particles, the random oscillations are primarily due to shear. The granular temperature due to shear in a rectangular bed is of the order of one cm^2/s^2.[26] This study suggests that the random oscillations of nanoparticles are primarily due to the collision with air

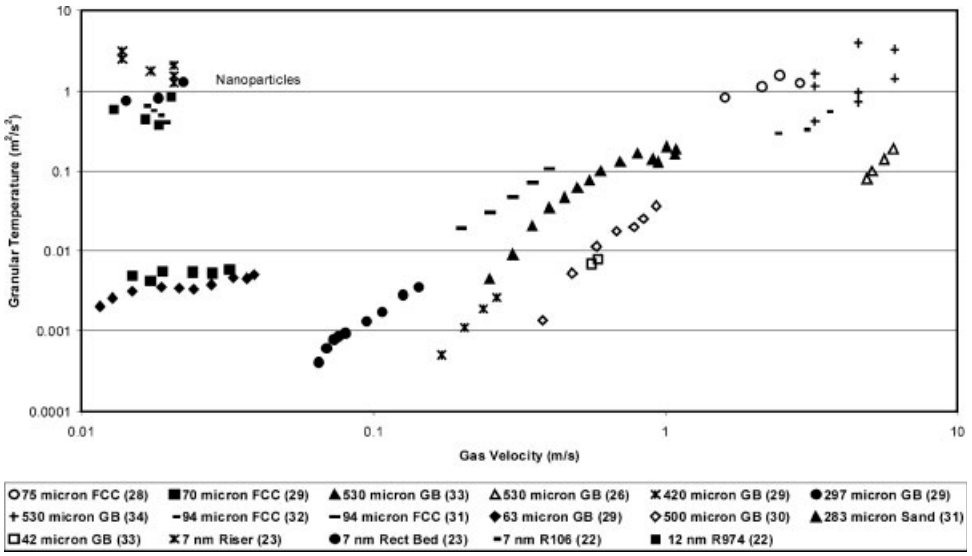

Figure 13. Effect of gas velocity on the granular temperature for particles of various sizes.

molecules, similar, but not identical to the Brownian motion of particles in a liquid.

Figure 13 shows the granular temperatures in this study compared to the measurements of granular temperature of large particles reported in literature.[23,28,29,30,31,32,33,34] Preliminary data were presented earlier at the 2004 Nanoscale Science and Engineering Grantee Conference Poster Session.[27] The earlier nanoparticle granular temperatures were similar, but not identical to those reported here.

Acknowledgment

The authors would like to acknowledge the contributions of Mr. Mayank Kashyap for his dedicated help during the execution of the experimental runs. His assistance is greatly appreciated. We also thank the National Science Foundation for the partial financial support through Grant #DMI0210400, and the co-principal investigators of this NSF project, Professors Hamid Arastoopour and Robert Pfeffer of N.J.I.T.

Notation

d = particle diameter, m
g = gravitational constant, m/s^2
G = solids-stress modulus, N/m^2
G' = modified solids-stress modulus, m^2/s^2
P_s = solids pressure, Pa
t = time, s
U_{mf} = minimum fluidization velocity, m/s
v = velocity, m/s
V = voltage, V
x = distance, m

Greek letters

β_B = gas-solid drag coefficient
ε_g = volume fraction of gas phase (or void fraction)
ε_S = volume fraction of solids phase (or solids-volume fraction)
θ = granular temperature, m^2/s^2
ρ_b = bulk density, kg/m^3
ρ_s = solids density, kg/m^3

Literature Cited

1. Jiradilok V, Gidaspow D, Kalra J, Damronglerd S, Nitivattanon S. Explosive dissemination and flow of nanoparticles. *Powder Technol*. 2006;164:33–49.
2. Kalra J. *Fluidization of Silica Nano-Size Particles in Circulating and Two Dimensional Fluidized Beds*. Illinois Institute of Technology; 2005. Masters Thesis.
3. Ratner M, Ratner D. *Nanotechnology A Gentle Introduction to the Next Big Idea*. Upper Saddle River, NJ: Prentice Hall; 2002.
4. Chaouki J, Chavarie C, Klvana D. Effect of interparticle forces on the hydrodynamic behavior of fluidized aerogels. *Powder Technol*. 1985;43:117–125.
5. Kunii D, Levenspiel O. Fluidization engineering. 2nd ed. Boston: Butterworth-Heinemann; 1991.
6. Wang Z, Kwauk M, Li H. Fluidization of fine particles. *Chem Eng Sci*. 1998;53:377–395.
7. Yao W, Guangsheng G, Fei W, Jun W. Fluidization and agglomerate structure of SiO_2 nanoparticles. *Powder Technol*. 2002;124:152–159.
8. Li H, Hong R, Wang Z. Fluidizing ultrafine powders with circulating fluidized bed. *Chem Eng Sci*. 1999;54:5609–5615.
9. Jung J, Gidaspow D. Fluidization of nano-size particles. *J Nanoparticle Res*. 2002;4:483–497.
10. Zhu C, Yu Q, Dave R, Pfeffer R. Gas fluidization characteristics of nanoparticle agglomerates. *AIChE J*. 2005;51:426–439.
11. Yang W. Fluidization of fine cohesive powders and nanoparticles - A Review. *J Chin Inst Chem Engrs*. 2005;36:1–15.
12. Huang C, Wang Y, Wei F. Multi-Stage Agglomerate Structure and Solids Mixing Behavior of Nano-Particle in Fluidized Bed. *AIChE Spring Meeting Conference Proceedings*. 2006;2:248c.
13. Valverde JM, Castellanos A, Lepek D, Quevedo J, Omosebi A, Dave R, Pfeffer R. The Effect of Gas Viscosity on the Agglomerate Particulate Fluidization State of Fine and Ultrafine Particles. *AIChE Spring Meeting Conference Proceedings*. 2006;2:248e.
14. Quevedo J, Flesch J, Pfeffer R, Dave R. Evaluation of Assisting Methods on the Fluidization of Agglomerates of Nanoparticles by Studying the Adsorption/Desorption Rate of Moisture. *AIChE Spring Meeting Conference Proceedings*. 2006;2:248d.
15. Sinclair JL. Hydrodynamic Modeling. In *Circulating Fluidized Beds*; Grace JR, Avidan AA, Knowlton TM, eds.; Blackie Academic and Professionals: London; 1997:149–180.
16. Gidaspow D. Multiphase Flow and Fluidization Continuum and Kinetic Theory Descriptions. New York: Academic Press; 1994.
17. Mutsers SM, Rietema K. The Effect of interparticle forces on the expansion of a homogeneous gas-fluidized bed. *Powder Technol*. 1977;18:239–248.
18. Rietema K, Piepers HW. The effect of interparticle forces on the stability of gas-fluidized beds - I. Experimental evidence. *Chem Eng Sci*. 1990;45:1627–1639.
19. Massoudi M, Rajagopal KR, Ekmann JM, Mathur MP. Remarks on the modeling of fluidized systems. *AIChE J*. 1992;38:471–472.
20. Chen L, Weinstein H. Measurement of normal stress and hindrance factor in a collapsing bed. *Chem Eng Sci*. 1994;49:811–819.
21. Gelderbloom SJ, Gidaspow D, Lyczkowski RW. CFD Simulations of bubbling/collapsing fluidized beds for three geldart groups. *AIChE J*. 2003;49:844–857.
22. Vasishta V. Hydrodynamics of *Fluidization and Settling of Silica Nanoparticles*. Illinois Institute of Technology; 2004. Masters Thesis.
23. Driscoll M. A study of the fluidization of fcc and nanoparticles in a rectangular bed and a riser. Illinois Institute of Technology, In Progress; 2007. PhD Thesis.
24. Jiradilok V. *Hydrodynamics of Fluidization of FCC Particles and Nanoparticles*. Chulalongkorn University; 2005. PhD Thesis.
25. Seo Y. *Fluidization of Single and Binary Size Particles*. Illinois Institute of Technology; 1985. PhD Thesis.
26. Tartan M, Gidaspow D. Measurement of granular temperatures and stresses in risers. *AIChE J*. 2004;50:1760–1775.
27. Gidaspow D, Arastoopour H, Pfeffer R, Vasishta V, Singh R, Jung J. Fluidization of Nanoparticles. *2004 Nanoscale Science and Engineering Grantee Conference*; 2004:274.
28. Gidaspow D, Huilin L. Equation of State and Radial Distribution Functions of FCC Particles in a CFB. *AIChE J*. 1998;44:279–293.
29. Cody G, Goldfarb D, Storch G, Norris A. Particle granular temperature in gas-fluidized beds. *Powder Technol*. 1996;87:211–232.
30. Campbell C, Wang D. Particle pressures in gas-fluidized beds. *J Fluid Mech*. 1991;227:495–508.
31. Polashenski W, Chen J. Normal solid stress in fluidized beds. *Powder Technol*. 1997;90:13–23.
32. Polashenski W, Chen J. Measurement of particle stresses in fast fluidized beds. *Ind Eng Chem Res*. 1999;38:705–713.
33. Jung J, Gidaspow D, Gamwo I. Measurement of two kinds of granular temperatures, stresses, and dispersion in bubbling beds. *Ind Eng Chem Res*. 2005;44:1329–1341.
34. Jung J. Design and understanding of turbulent, bubbling and slurry bubble column reactors. Illinois Institute of Technology; 2003. PhD Thesis.

Appendix A: Shock Wave Theoretical Background

Theoretical background

The proposed experiment is based on the derivation of the granular flow of solids presented in Gidaspow.[16] The derivation is initiated by stating the 1-D mass and momentum balances for the granular flow of solids. The momentum balance is based on a positive upward x-direction, and gravity is directed negative in the downward direction.

Mass balance for the solids phase

$$\frac{\partial(\rho_b)}{\partial t}+\frac{\partial}{\partial x}(\rho_b v_s)=0 \tag{A1}$$

Momentum Balance for the solid phases

$$\frac{\partial(\rho_b v_s)}{\partial t}+\frac{\partial}{\partial x}(\rho_b v_s v_s)=-\frac{\partial P_s}{\partial x}+g(\rho_s-\rho_g)\varepsilon_s+\beta_B(v_s-v_g) \tag{A2}$$

Now, the definition of the solids-stress modulus and the chain rule are utilized

$$\frac{\partial P_s}{\partial x}=\frac{\partial P_s}{\partial \varepsilon_s}\cdot\frac{\partial \varepsilon_s}{\partial x}=G\cdot\frac{\partial \varepsilon_s}{\partial x} \tag{A3}$$

Substitution of this relationship into the momentum balance, rearranging and substituting these equations into in matrix form yields

$$\begin{pmatrix}\frac{\partial\rho_b}{\partial t}\\ \frac{\partial v_s}{\partial t}\end{pmatrix}+\begin{pmatrix}v_s & \rho_b\\ \frac{G'}{\rho_b} & v_s\end{pmatrix}\begin{pmatrix}\frac{\partial\rho_b}{\partial x}\\ \frac{\partial v_s}{\partial x}\end{pmatrix}=\begin{pmatrix}0\\ \frac{\varepsilon_s(\rho_s-\rho_g)g}{\rho_b}+\frac{\beta_B(v_s-v_g)}{\rho_b}\end{pmatrix} \tag{A4}$$

The characteristic determinant for these equations is

$$\begin{vmatrix}v_s-\lambda & \rho_b\\ \frac{G'}{\rho_b} & v_s-\lambda\end{vmatrix}=0 \tag{A5}$$

The characteristic direction for a fluidized system of particles is

$$\lambda=\frac{dx}{dt}=v_s\pm\sqrt{\frac{G}{\rho_s}}=v_s\pm\sqrt{G'} \tag{A6}$$

where

$$G'=\frac{G}{\rho_s}$$

Based on this characteristic equation for 1-D flow, the modified solids-stress modulus G′, may be back calculated from the solids velocity and the characteristic velocity. The analysis may be further simplified by assuming solids velocity is negligible. This assumption can be justified since the fluidization velocity was on the order of 0.01 m/s vs. the wave velocity that was on the order of 1 m/s, and the fluidized bed was maintained at a constant height (zero net bed velocity) prior to the induced wave to minimize the overall bed velocity.

Now, since nanoparticles tend to fluidize in a dilute solid-volume fraction regime, the particulate ideal equation of state from kinetic theory of granular solids will apply. Therefore, by definition

$$P_s=\rho_s\varepsilon_s\theta \tag{A7}$$

The ideal particulate equation of state strictly applies for dilute systems. This requirement is consistent with fluidized nanoparticle systems that have been experimentally verified to operate at dilute solids-volume fractions.[1,2,9,22] Now, recalling the definition of the modified solids-stress modulus

$$G'=\frac{G}{\rho_s}=\frac{1}{\rho_s}\left(\frac{\partial P_s}{\partial \varepsilon_s}\right) \tag{A8}$$

Inserting the ideal equation of state into this equation yields

$$G'=\frac{1}{\rho_s}(\rho_s\theta)=\theta \tag{A9}$$

Now, equating the characteristic velocity with this equation yields

$$\left(\frac{dx}{dt}\right)=\sqrt{G'}=\sqrt{\theta} \tag{A10}$$

Therefore, the characteristic velocity from the wave experiments can be used to calculate the granular temperature and the modified solids-stress modulus.

Manuscript received Jun. 24, 2006, and revision received Mar. 9, 2007.